EARTH SURFACE PROCESSES AND LANDFORMS
Earth Surf. Process. Landforms (2016)

Published online in Wiley Online Library
(wileyonlinelibrary.com) DOI: 10.1002/esp.3916

Selective organic carbon losses from soils by sheet erosion and main controls

Daniel Müller-Nedebock,[1] Pauline Chivenge[1,2] and Vincent Chaplot[1,3]*

[1] School of Agricultural, Earth and Environmental Sciences, Centre for Water Resources Research, University of KwaZulu-Natal, Scottsville, South Africa
[2] ICRISAT, Matopos Research Station, P.O. Box 776, Bulawayo, Zimbabwe
[3] Institut de Recherche pour le Développement (IRD), Laboratoire d'Océanographie et du Climat (LOCEAN), UMR 7159, IRD/UPMC/CNRS/MNHN, Institut Pierre Simon Laplace, Paris, France

Received 20 February 2015; Revised 25 January 2016; Accepted 26 January 2016

*Correspondence to: Vincent Chaplot, Institut de Recherche pour le Développement (IRD), Laboratoire d'Océanographie et du Climat (LOCEAN), UMR 7159, IRD/UPMC/CNRS/MNHN, Institut Pierre Simon Laplace, 4, place Jussieu 75252, Paris Cedex 05, France. E-mail: Vincent.Chaplot@ird.fr

ESPL
Earth Surface Processes and Landforms

ABSTRACT: Although the impact of sheet erosion on the selective transportation of mineral soil particles has been widely investigated, little is yet known about the specific mechanisms of organic carbon (OC) erosion, which constitutes an important link in the global carbon cycle. The present study was conducted to quantify the impact of sheet erosion on OC losses from soils. Erosion plots with the lengths of 1- and 5-m were installed at different topographic positions along a hillslope in a mountainous South African region. A total of 32 rainfall events from a three years period (November 2010 up to February 2013), were studied and evaluated for runoff (*R*), particulate and dissolved organic carbon (POC_L and DOC_L). In comparison to the 0–0·05 m bulk soil, the sediments from the 1-m plots were enriched in OC by a factor 2·6 and those from the 5-m long plots by a factor of 2·2, respectively. These findings suggest a preferential erosion of OC. In addition, total organic carbon losses (TOC_L) were incurred mainly in particulate form (~94%) and the increase in TOC_L from $14{\cdot}09 \pm 0{\cdot}68$ g C m^{-1} yr^{-1} on 1-m plots to $50{\cdot}03 \pm 2{\cdot}89$ g C m^{-1} yr^{-1} on 5-m plots illustrated an increase in sheet erosion efficiency with increasing slope length. Both TOC_L and sediment enrichment in OC correspondingly increased with a decrease in soil basal grass cover. The characteristics of rainstorms had no significant impact on the selectivity of OC erosion. The results accrued in this study investigating the links between sheet erosion and OC losses, are expected to be of future value in the generation of carbon specific erosion models, which can further help to inform and improve climate change mitigation measures.

KEYWORDS: land degradation; climate; carbon cycle; grassland; Africa

Introduction

Soils, which sequester atmospheric carbon (CO_2), by means of retaining and absorbing the plant residue of photosynthesizing plants, have been shown to contain more than half the carbon in terrestrial ecosystems (Schlesinger and Andrews, 2000). Hence, by having the potential to offset the current influx of anthropogenic CO_2 emissions (Lal, 2004), soils, through their sequestration properties, could provide a possible solution for global warming. For instance, soil organic matter (SOM), which soil organic carbon (SOC) constitutes the bulk of, provides the soil with essential plant nutrients, improves soil texture, acts as a natural buffer against compaction, enhances soil water retention capacity and provides energy for soil biota (Pimentel *et al*., 1995; Biggelaar *et al*., 2001; Lal, 2003).

Soil erosion by water is a pervasive process that involves the detachment and transport of soil particles by raindrop impact and overland flow (Chaplot & Le Bissonnais, 2003; Chaplot & Poesen, 2012; Kinnell, 2004). It is a highly selective process, resulting in the translocated sediments to have starkly differing properties to the soils that they emanate from (Mitchell *et al*., 1983; Govers, 1985; Hairsine and Rose, 1991). Once in suspension, the finer soil fractions, composed mainly of the clays, tend to be transported across greater distances in contrast to the coarser fractions, which are generally composed of sand (Poesen and Savat, 1980; Govers, 1990). However, under certain circumstances coarser particles may be preferentially eroded as a result of rolling (Asadi *et al*., 2011).

Partly owing to its light nature and the complex but reversible associations with the mineral soil matrix, SOC seems to be particularly vulnerable to the mechanisms of water erosion, thus making possible preferential accelerated carbon losses from soils (Gregorich *et al*., 1998; Jacinthe and Lal, 2001; Chaplot *et al*., 2005; Behre *et al*., 2007; Nadeu *et al*., 2011, 2012; Van Hemelryck *et al*., 2011; Mchunu and Chaplot, 2012; Hoffmann *et al*., 2013). The annual SOC stock depletion rates, calculated by using the 0–0·3 m soil horizon, were shown to vary amongst different environments. In Spain, Rodríguez-Rodríguez *et al*. (2004, reported depletion rates of 0·01% in the 0–0·3 m soil horizon. In India SOC stocks were found to deplete at a rate of 0·5% (Cogle *et al*., 2002), 1·3% in Laos (Chaplot *et al*., 2007), and in a study conducted in

Burkina Faso utilizing 22·2-m long plots, depletion rates as high as 16% were observed (Roose, 1978). Moreover, in a Kenyan study conducted by Boye and Albrecht (2006, it was observed that sediments eroded from 1-m plots were enriched by a factor of 3·3 in organic carbon (OC). The OC enrichment ratio (ER) was 4·3 for a biennial cotton/corn rotation fields in a study performed in Burkina Faso (Bilgo *et al.*, 2006), ranging between 4·3 and 4·8 for sandy soils in South Africa, measured with 10 m long plots (Mchunu *et al.*, 2011) and as high as 10 in the sandy, semi-arid environment of Mali (Drissa *et al.*, 2004). In their review of tropical and Mediterranean soils, Roose and Barthès (2006 pointed to ER values in the range between 0·5 and 14, with values below 1·1 occurring for tilled soils, while values over 3·0 were calculated for natural vegetation (e.g. forest, savanna, or fallow). While the preferential export of SOC from soils by water erosion has been observed and acknowledged, little is known about the main mechanisms and controlling actions. Schiettecatte *et al.'*s (2008 laboratory simulated rainfall study, investigating rain-impacted-flow (RIF), revealed that high intensity storms are less preferentially selective regarding the transportation of OC, than low intensity events. Can these results, however, be applied to field conditions, in particular when the natural environment and large areas are considered (Wang *et al.*, 2010)? Do the soil properties, land use and management, topography and terrain morphology not also affect the selectivity of OC erosion by water? Moreover, what would the impact be considering a combination of these respective factors? These important questions remain largely unanswered.

The main objective of this study was to further improve the understanding of how soil erosion mechanisms affect the global carbon cycle and also: (i) to quantify the extent to which sheet erosion controls OC movement; (ii) to identify the principal mechanisms of selection involved in the erosion of SOC erosion; (iii) to determine the main environmental and soil factors that control SOC erosion.

The research of this study was performed in the hillslopes of KwaZulu-Natal, South Africa, where subsistence farmers, resort to cultivating crops on generally steep slopes and in degraded soils for their survival.

In order to identify the main selection mechanisms involved in the erosion of SOC and the pertaining soil and environmental factors, 1- and 5-m long erosion plots were installed at different topographic positions along a hillslope, characteristic of varying parent material, soil properties and basal grass cover.

Materials and Methods

Study area

The research was conducted in the 23 ha catchment of a rural, communal settlement by the name of Potshini (longitude: 29·36°; latitude: 28·82°), situated in the greater Thukela River basin (30 000 km^2) of KwaZulu-Natal, South Africa. The land is utilized by local smallholder farmers for subsistence crops and communal grazing land. Rills and gullies are common throughout the landscape of the catchment (Chaplot, 2013), which is an indicator of poor grazing management and practice. Potshini is characterized by a tropical, sub-humid climate with a summer rainfall pattern (September–March). The geology of the area is characterized by an irregular sequence of fine grained sandstone, shale, siltstone and mudstone spread out horizontally, with erratic intrusions of Karoo dolerite sills. Acrisols (WRB, 2006) are the main soils found in the area, which are generally deep at the footslope and shoulder, while shallow at midslope positions. The topography of the 23 ha catchment ranges from gentle to moderate, with an average slope gradient of 15·3°. The hillslope chosen for the experiment has a maximum slope gradient of 29°. The altitude within the catchment ranges from 1381 m to 1492 m above sea level.

The meteorological data was obtained from the Bergville weather station, situated 10 km east of the study site. According to the data, the mean annual temperature (MAT) of the area is 13 °C, the mean annual precipitation (MAP) is 684 mm and the potential evaporation is 1600 mm yr^{-1}. Meteorological records spanning across a 30 year period, obtained from the national data base, show that rainfall events with a maximum half hour intensity of 49 mm h^{-1} (I_{30}) have a probability of re-occurring every two years, with a 90% probability occurrence between 37 and 61 mm h^{-1}. The re-occurrence period for a rainfall event with the maximum half hour intensity of 76 mm h^{-1} is 10 years and the probability for a 115 mm h^{-1} intensity rain is 100 years.

Experimental design

Because the level of contribution of the main sheet erosion mechanisms, i.e. splash and RIF, to SOC erosion is expected to depend on spatial scale and terrain and soil characteristics, plots of different length were installed in a typical catena from the grassland landscape at different topographic conditions with varying soils and levels of grass degradation. Five positions were selected with the following characteristics: Footslope (F), characterized by a gentle slope and deep acrisols with high basal grass cover; Midslope (M), characterized by a steep slope and shallow acrisols and diminished grass cover; Terrace (T), marked by a flat gradient and shallow clayey acrisols; Shoulder dolerite (SD), characterized by deep reddish clayey acrisols and high basal grass cover; Shoulder sandstone (SS) characterized by deep yellowish sandy acrisols and an intermediate basal grass cover (Figure 1; Table I).

Experimental erosion plots of 1- and 5-m long (1 × 1 m^2 and 2 × 5 m^2, respectively) were installed at each of these positions to identify the main erosive mechanisms involved in selective translocation of SOC, and to further identify possible factors control SOC erosion. At each hillslope position there were three 1-m long plots and two 5-m long erosion plot replicates installed. Plots were orientated in the direction of the natural slope gradient. Steel sheets were used as plot boundaries and anchored in the soil at a depth of 0·1 m. At the foot-end of every erosion plot, PVC (polyvinyl chloride) piping connected the erosion plot to a reservoir used to collect runoff and sediments, which were stored in a collector-bucket. Water erosions preferential selection of SOC translocation was assessed individually for each plot length by comparing the OC content of the eroded sediments to that of the bulk soil.

Additionally, the runoff volume (R) in the plot was evaluated after each storm event. An aliquot of the runoff was dried and weighed. The weight of sediments was used to compute the sediment concentration in runoff (SC), a key variable in estimating the total soil losses (SL) and soil losses per plot, per meter width, which was calculated as a product of R and SC divided by the plot width (i.e. 1 for 1 m^2 plots and 2 for 10 m^2 plots).

Field measurements were performed subsequent to the 32 erosive rainfall events of two hydrological years, which occurred from November 25, 2010 up until February 8, 2013. Since, none of the runoff plots displayed any significant features of linear erosion or soil cracking, the measurements were assumed to have been made under steady-soil-state conditions. Hence the observed soil and carbon losses are considered to be the result of strictly RIF action, and sheet erosion mechanisms.

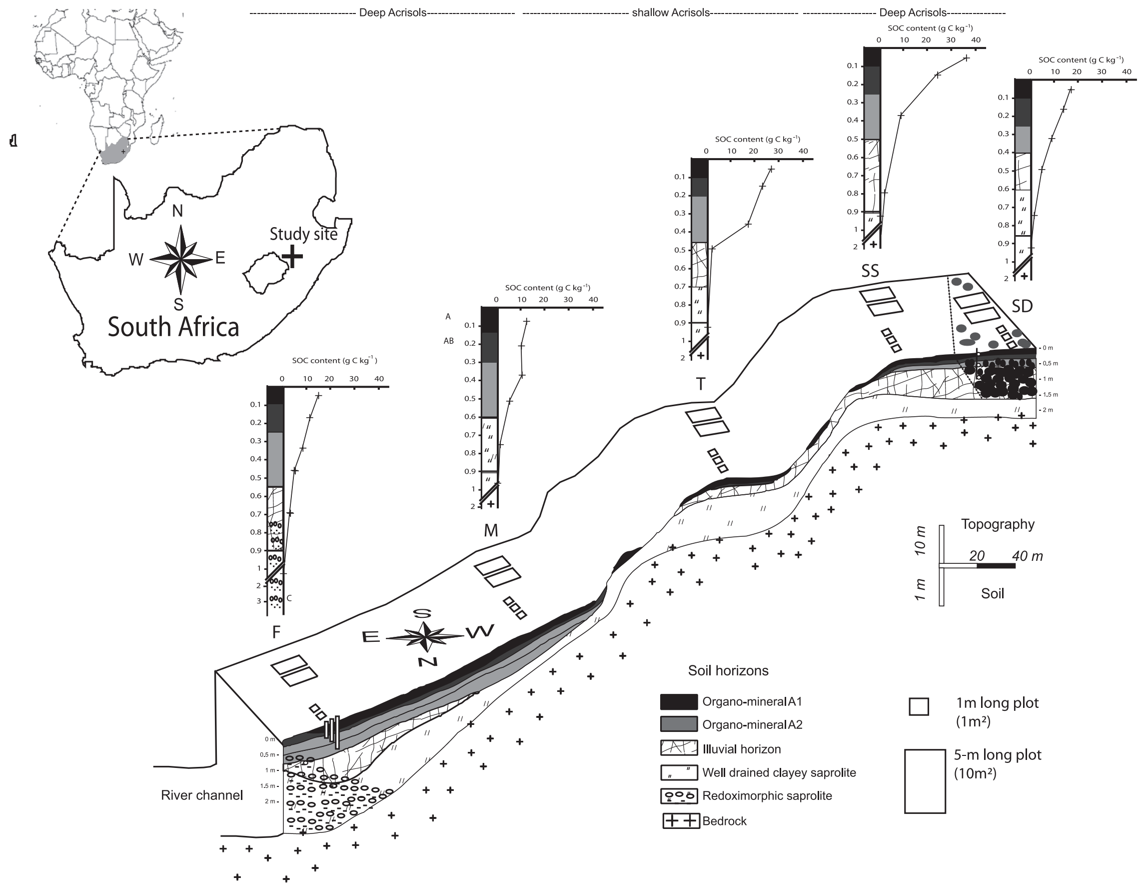

Figure 1. Diagram depicting a cross-section profile of the study hillslope (Potshini research catchment of South Africa) showing the position of the 1-m and 5-m long plots at the study landscape positions: footslope (F), midslope (M), terrace (T), shoulder sandstone (SS) and shoulder dolerite (SD). Soil carbon data were extracted from Dlamini *et al.* (2011.

Table I. Soil and environmental characteristics for the different hillslope positions (Figure 1)

Position	Crust (%)	Cov (%)	Clay (%)	S	ρ_b (g cm^{-3})	SOC_{C2} (g C kg^{-1})	SOC_{C5} (g C kg^{-1})	SOC_{S2} (g C kg^{-1})	SOC_{S5} (g C kg^{-1})
Footslope	4	96	28	23	1·25	42·9	23·8	1·073	1·488
Midslope	48	52	27	29	1·33	18·8	16·5	0·500	1·097
Terrace	2	98	40	10	1·13	45·0	26·1	1·017	1·475
Shoulder Dolerite	6	94	54	15	1·02	40·0	35·2	0·816	1·795
Shoulder Sandstone	17	83	31	19	1·12	30·1	23·3	0·674	1·305
Mean	17	85	36	20	1·17	35·4	24·9	0·816	1·432

Note: Crust, represents the proportion of the soil surface with crusts; Cov, grass basal cover; Clay, clay content of the top-soil; S, mean slope gradient; ρ_b, top-soil bulk density; SOC_{C2} and SOC_{C5}, soil organic carbon content of the 0–0·02 m and 0–0·05 m soil layers; and SOC stocks SOC_{S2} and SOC_{S5}.

The analytic methods

The machine used for estimating the total organic carbon content (TOC_C) in the bulk soil and in sediments was a LECO CNS-2000 Dumas Dry Matter Combustion Analyzer (Leco Corp., St Joseph, MI, USA). The analyses were performed on air-dried bulk top-soil samples and air-dried sediment samples. Organic materials in soils and sediments range from simple sugars and carbohydrates to the more complex proteins, fats, waxes, and organic acids, and are mostly found in particulate (diameter < 0·45 μm) form. The stock of organic carbon in soils (SOC_S) was determined from the product of soil bulk density, which was obtained from core sampling and oven drying at 105 °C, the thickness of the soil layer and the content of soil organic carbon (SOC_C) of that layer (expressed in kg C m^{-2}). Two soil layers, the 0–0·02 m layer and the 0–0·05 m, were considered for the analysis. Three samples from each layer were taken on all five studied hillslope position, resulting in total of 30 soil samples.

The total particulate organic carbon losses (POC_L) were calculated by the product of runoff (R) and particulate organic carbon content (POC_C).

The content of total dissolved (< 0·45 μm) organic carbon in runoff (DOC_C) was estimated using a Shimadzu TOC-5000 analyzer with an ASI-5000 autosampler and Balston 78–30 high purity gas generator (Shimadzu, Tokyo, Japan). Filtered samples of 0·45 μm were analyzed immediately after sampling or, in the event of backlog, refrigerated at 4 °C until analysis could proceed. Standard solutions of 0, 10, 50 and 100 ppm carbon were made, using 0, 1, 5 and 10 ml of stock solution, prepared by dissolving 2·125 g of the oven dried reagent 'potassium hydrogen phthalate' (C8H5KO4) in 1000 ml of distilled water.

POC_C and DOC_C were estimated for five sediment samples chosen from five corresponding rainfall events each year between 2010 and 2013, from both, the microplots ($n = 15$) and plot ($n = 10$) replicates, resulting in a total of 375 samples. The events were chosen, as they represented a good average of the diversity of all the natural events that occurred in the study area from the onset of the rain season until its end, with a rainfall intensity range from to 6 to 164 mm h^{-1}. The total POC_L were calculated by the product of R and POC_C while dissolved organic carbon losses (DOC_L) were then calculated as a product of R and DOC_C. In order to compare the data from the different plots on equivalent terms, DOC_L and POC_L were subsequently transformed into delivery fluxes, which were expressed as per meter contour width.

Total organic carbon losses (TOC_L) were then calculated as the sum of DOC_L and POC_L.

Finally, the ER (i.e. the ratio of the concentration of OC in the eroded sediment to its concentration in the original soil) was calculated to assess the selectivity of OC erosion. Because SOC_c decreases significantly from top-soil to deep in the soil profile, the thickness of the top-soil layer considered for ER estimation is critical. Here we considered the 0–0·02 and the 0–0·05 m layers with ER_2 considering the 0–0·02 m layer and ER_5 the 0–0·05 m layer.

Environmental and soil controls

Rainfall event characteristics; rainfall amount (RA) per event, maximum six-minute rainfall intensity (RI_6), three-day antecedent rainfall (AR_3) and cumulative annual rainfall (CR) from the onset of the first rainy season were logged using an automatic rain gauge, located at the T hillslope position. Based on the 32 study, erosive rainfall events (from November 25, 2010 up until February 8, 2013), the cumulative rainfall over 2010–2011 was 685 mm. It decreased to 331 mm over 2011–2012 and was 702 mm during 2012–2013. The maximum event RA was 139 mm and was recorded twice on December 14, 2010 and September 13, 2012. The average RA was 53 mm and RA over 100 mm occurred eight times. The average RI_6 was 45 mm h^{-1} with a maximum of 164 mm h^{-1} observed on January 20, 2012. Two events with RI_6 over 100 mm h^{-1} were recorded on February 2, 2011 (102 mm h^{-1}) and October 25, 2012 (134 mm h^{-1}).

The following site-specific characteristics were also considered: mean slope gradient (S), percentage of soil surface crusting (Crust), basal soil cover (Cov), top-soil clay content (Clay), bulk soil density (ρ_b), SOC content (SOC_{C2} for the 0–0·02 m layer; SOC_{C5} for the 0–0·05 m layer), and associated SOC stocks (SOC_{S2}; SOC_{S5}). The value for S was assessed for each plot using a laser theodolite. Soil crusting and cover were determined following Dlamini *et al.*'s (2011 methodology, which entails the use of distance meter laser equipment (Leica Disto. Pro, laser class 2–635 nm, LEICA geosystems AG, CH-9435 Heerbrugg, Switzerland) mounted at a height of 1·0 m above the plot to evaluate the occurrence of bare soil or grass on a 0·05 m grid. The particle size distribution of the 0–0·05 m bulk soil was determined using Gee and Bauder's (1986 pipette method.

Statistical analysis

Pearson r correlations were used to investigate the correlations between the study variables in the dataset. In addition, a principal component analysis (PCA) was used to evaluate the relationship between the erosion variables and the soil and environmental factors. During the PCA the variables are converted into the 'so-called' factors, or principal components (PCs), which are linear combinations of the actual variables. There PCs are not correlated with each other (i.e. they are orthogonal) and together they can be used to explain certain data variance (Jambu, 1991). In this tool, the first principal component (PC1) explains the highest percentage of the system variability, while the second principal component (PC2) corresponds to a lower proportion of the variance. In addition, paired t-test were used to compare each study variable to the mean result from the 1- and 5-m long plots. Using a null hypothesis means that the two populations are equal. The 0·05 level was implemented in this study in order to reject the null hypothesis in favor of an alternative hypothesis, which suggests that the two treatments have different means.

Results

Spatial variations of soil organic carbon (SOC) content and SOC stocks across the study hillslope

The average SOC_C in the top 0·02 m layer of the soil (SOC_{C2}), was 35·4 g C kg^{-1}, which was 30% greater than in the upper 0·05 m SOC_{C5} (24·9 g C kg^{-1}; Table I). The average SOC_S was 0·816 kg C m^{-2} for the 0–0·02 m layer and increased to 1·432 kg C m^{-2} for 0–0·05 m.

The greatest SOC_C was found at the SD position (35·2 g C kg^{-1} at SD in the upper 0·05 m, SOC_{C5}) while the lowest value (16·5 g C kg^{-1} for SOC_{C5}) was found at the M position. The soils at both the SS and T positions showed a drastic decrease in SOC_C with increasing soil depth, which contrasted with the results incurred at the F, M and SD positions (Figure 1). SOC_{S5} values ranged from 1·097 kg C m^{-2} at M to 1·795 g C m^{-2} at SD (Table I).

Rate of soil and SOC erosion and main controls

Slope length

The mean event runoff (R) across all hillslope positions decreased from 13·8 l m^{-1} with a standard error of ±0·63 l m^{-1} on 1-m plots to 57·8 ± 3·2 l m^{-1} on 5-m plots (Table II), which represented a 318% increase, a significant difference at $P < 0·05$. By contrast, the average event SC was 7·5% lower for the 5-m plots (1·20 ± 0·07 g l^{-1}) than for the shorter plots (1·29 ± 0·06 g l^{-1}). The mean event SL increased with slope length from 23·2 ± 1·1 on 1-m to 97·6 ± 5·5 g m^{-1} on 5-m plots, which corresponded to a 321% increase, significant at $P < 0·05$. The three-year cumulative SL, which was computed from all the 32 storm events and the plots replicates, was 741 g m^{-1} on 1-m plots and 2834 g m^{-1} on 5-m plots (i.e. a 182% difference), which corresponded to average yearly SL of 247 g m^{-2} yr^{-1} on 1-m plots and 189 g m^{-2} yr^{-1} on 5-m plots. SL were the lowest (1501 g m^{-1}) at the F position and were the highest (4317 g m^{-1}) at M (Figure 2).

Peculiarly, the total POC_C decreased with an increase in slope length from 62·8 ± 2·9 g C kg^{-1} on 1-m to 51·6 ± 2·9 g C kg^{-1} on 5-m plots and a similar trend occurred for DOC_C: i.e. a decrease from 11·9 ± 0·5 mg C l^{-1} at 1-m to 8·6 ± 0·5 mg C l^{-1} at 5-m plots (Table II). In average, event POC_L were 1·23 ± 0·06 g C m^{-1} on 1-m and 4·43 ± 0·27 g C m^{-1} on 5-m, a 260% increase, significant at $P < 0·05$ and the resulted average yearly carbon losses were 13·16 ± 0·68 g C m^{-1} yr^{-1} on 1-m and 47·30 ± 2·89 g C m^{-1} yr^{-1} on 5-m plots. In the mean time, the average DOC_L was 87·5 ± 3·9 mg C m^{-1} yr^{-1} on 1-m plots and 256·0 ± 14·3 mg C m^{-1} yr^{-1} on 5-m plots, a 192% difference significant at $P < 0·05$. The resulting average TOC_L (i.e. the sum of DOC_L and POC_L) were 14·09 ± 0·68 g C m^{-1} yr^{-1} on 1-m plots and 55·03 ± 2·89 g C m^{-1} yr^{-1} on 5-m plots, a 290% increase, which was significant at $P < 0·05$.

Table II. Summary statistics for event runoff (R), sediment concentration (SC), soil losses (SL), particulate organic carbon content and losses (POC_C; POC_L), dissolved organic carbon content and losses (DOC_C; DOC_L), sediment enrichment ratio (ER) in particulate soil organic carbon compared to the bulk 0–0·02 m (ER_2) and 0–0·05 (ER_5) soil, and computed from the 1- and 5-m long plot replicates and the 32 study storm events which occurred during the three-years period

	R		SC		SL			POC_C		POC_L			DOC_C		DOC_L			ER_2		ER_5	
	(l m^{-1})		(g l^{-1})		(g m^{-2})		(g m^{-1})	(g C kg^{-1})		(g C m^{-2})		(g C m^{-1})	(mg C l^{-1})		(mg C m^{-2})		(mg C m^{-1})				
	1 m	5 m	1 m	5 m	1 m	5 m	5 m	1 m	5 m	1 m	5 m	5 m	1 m	5 m	1 m	5 m	5 m	1 m	5 m	1 m	5 m
Mean	13·8	57·9	1·29	1·20	23·2	19·5	97·6	62·8	51·6	1·23	0,98	4·43	11·9	8·6	87·5	72·2	256·0	1·9	1·6	2·6	2·2
Median	7·3	8·7	0·55	0·52	4·2	0·7	3·5	58·0	53·5	0·20	0·04	0·18	6·6	8·1	26·2	2·8	2·3	1·7	1·4	2·3	2·1
Minimum	0·0	0·0	0·0	0·0	0·0	0·0	0	10·2	12·5	0·01	0·01	0·01	0·0	0·2	0·0	0·0	0	0·3	0·3	0·5	0·4
Maximum	96·2	415·3	14·1	10·4	495	280	1402	276	210	21·88	15·26	76,30	156	22·7	1443	657	3272	12·9	7·0	14·7	9·0
Standard error	0·63	3·2	0·06	0·07	1·1	1·1	5·5	2·9	2·9	0·06	0·05	0·27	0·5	0·5	3·9	11·0	14·3	0·1	0·1	0·1	0·1

The greatest cumulative runoff for the three-year period from 1-m plots occurred at the M position, while the greatest R on 5-m plots occurred at the SD position, closely followed by M (Figure 2). On both the 1- and 5-m plots, the greatest cumulative SL were observed at M (1204 and 4318 g m^{-2} yr^{-1}, respectively). The greatest increase in SL with increasing slope length occurred at SD (617 g m^{-1} on 1-m versus 3753 g m^{-1} on 5-m, which corresponded to a 508% difference), whilst the lowest difference was observed at the T position (741 versus 2256 g m^{-1}, a 204% increase). In the mean time, the M position exhibited a 258% increase, F, a 202% and SS a 309% increase (Figure 2).

The three-years cumulative TOC_L from 1-m plots ranged from 27·3 g C m^{-2} at F to 50·0 g C m^{-2} at T, a 83% difference, which was significant at $P < 0·05$. TOC_L ranked second at SS (30·6 g C m^{-2}), third at SD (43·3 g C m^{-2}) and fourth at M (46·1 g C m^{-2}). TOC_L increased rapidly for all hillslope positions during the initial part of the first rainy season and then plateaued before revealing another, although less acute increase during the second rainy season. The 5-m plots exhibited a similar behavior, i.e. highest TOC_L during the first rainy season, and lowest cumulative losses (56·2 g C m^{-2}) at the F position. However, the greatest carbon losses occurred at M (200·0 g C m^{-2}) (Figure 2). The TOC_L increase from 1- to 5-m plots ranged between 107 and 349% with the highest values being found under SD, SS and M while lowest values occurred at T and at F (Figure 2).

Impact of the other selected factors

The values of R, SC and SL positively correlated with event RA, CR and RI_6 but negatively correlated with AR_3 (Table III). In addition, while SC and SL increased with the increase in soil crusting (Crust) and slope gradient (S), it decreased with increasing soil basal cover (Cov). Interestingly, SC increased with increasing SOC_C and SOC_S only at the shortest slope.

TOC_L from 1-m plots increased significantly with Crust ($r = 0·65$), Clay ($r = 0·53$), SOC_{C5} ($r = 0·53$), RA ($r = 0·45$), RI_6 ($r = 0·45$), and CR ($r = 0·45$), and decreased correspondingly with increasing AR_3 ($r = -0·45$) and ρ_b ($r = -0·44$) (Table III). On the 5-m long plots, TOC_L proved to be governed by similar controlling variables, the only outlier being a significant correlation with S ($r = 0·30$) (Table III). The correlation coefficients were however much lower among the study variables: CR ($r = 0·33$), RI_6 ($r = 0·33$), AR_3 ($r = -0·33$), SOC_C and SOC_S (e.g. $r = -0·32$ for SOC_{C2}), Clay ($r = -0·31$) and Cov ($r = -0·20$) (Table III).

Selectivity of SOC erosion

Compared to the original bulk soil, the eroded soil material appeared to be systematically enriched in OC. The greatest enrichments occurred on the 1-m long plots, where an ER of 1·86 (i.e. a 86% enrichment of the sediments in OC) was observed, when considering the 0–0·02 m layer, and an ER of 2·57 when the 0–0·05 m layer was considered (Table II). For the 5-m plots, the ER decreased to 2·17, when comparing it to the top 0·05 m of soil and to 1·61 for the top 0·02 m.

ER_2 on 1-m plots was most affected by soil ρ_b, followed by Clay, Crust and Cov with the ER correspondingly increasing with an increase in ρ_b ($r = 0·62$) and decreasing Clay ($r = -0·46$), Crust ($r = -0·33$), SOC_{C2} ($r = -0·32$) and Cov ($r = -0·30$) (Table III). A similar pattern was observed for ER_5 (Table III).

On the 5-m plots, both ER_2 and ER_5 increased with increasing S and decreasing SOC_C, Cov and Clay (Table III).

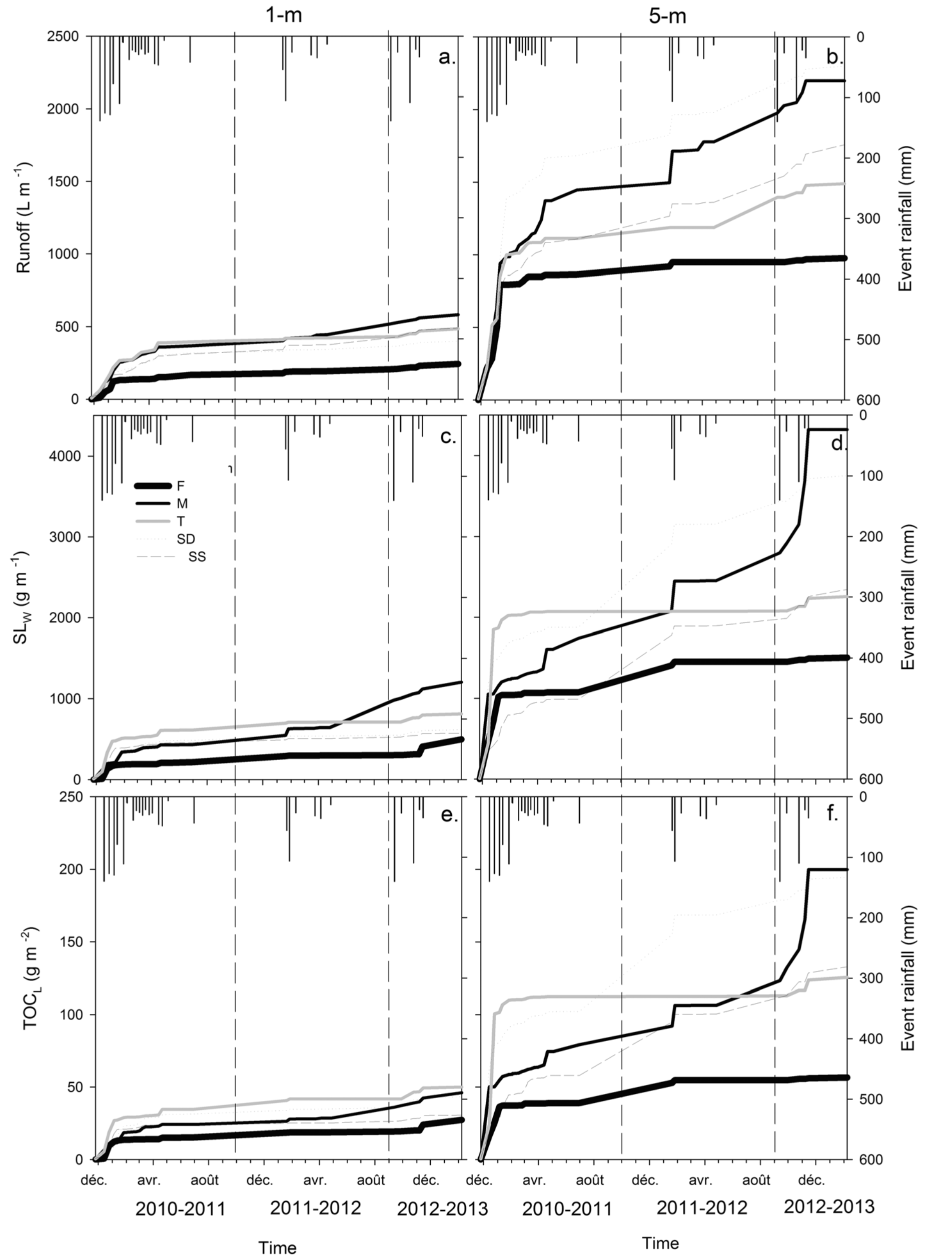

Figure 2. Cumulative runoff (R) (a) and (b); soil losses per meter width (SL_W) (c) and (d); and total organic carbon losses (TOC_L) (e) and (f) from 2010 to 2013 from the 1- and 5-m long plots (left and right, respectively) and installed at the different slope positions: footslope (F), midslope (M), terrace (T), shoulder sandstone (SS) and shoulder dolerite (SD).

The PCA generated using the soil and environmental controls explained 75% of the total data variance with the PC1 explaining 41% and PC2, 34% (Figure 3). PC1 revealed negative coordinates for Clay, SOC_C, SOC_S and Cov whilst S, ρ_b and Sand had positive coordinates. PC1 can thus be interpreted as an axis opposing clayey-organic and non-degraded soils from smooth slopes to degraded sandy soils from steep slopes. PC2 opposed intense storm events (high RI_6, CR and CR) from the end of the rainy season to low intensity storms resulted by the early rainy seasons. ER_2 and ER_5 were the most correlated to PC1, with greater carbon enrichment in the eroded sediments occurring for clayey-organic and non-degraded soils. The very lowest coordinates for ER_2 and ER_5 on PC2 come as a confirmation for the limited impact that the climatic variables had on the selectivity of carbon erosion. There was a tendency for soil losses per meter width (SL_W) to increase with increasing rainfall event intensity, but to decrease with three-days antecedent moisture. SL_W also increased correspondingly with an increase in slope steepness and soil crusting. TOC_L positively correlated with PC2 only, meaning that rainfall variables had a greater impact on soil carbon losses than soil variables.

Discussion

Significance of soil erosion and the main controlling variables in the grassland hillslope study

In average over the study period of three years the cumulative soil losses from the grassland study's 5-m long plots ranged between 1501 and 4317 g m^{-1}, i.e. 500·3 and 1439 g m^{-1} yr^{-1} or 5·00–14·39 Mg ha^{-1} yr^{-1}), depending on the landscape position (Figure 2). This was comparatively high, as Roose and Barthès (2006 in their review of soil erosion on rangeland soils showed rates between 0·7 and 1·8 Mg ha^{-1} yr^{-1}, the highest value here were found for steep sloped terrain and low basal grass cover. The soil erosion range at the study site

Table III. Pearson *r* coefficient between environmental and soil characteristics, and losses from 1-m (a) and 5-m (b) long plots and across all landscape positions

	RA	RI_6	AR_3	CR	*S*	Crust	Cov	Clay	ρ_b	SOC_{C2}	SOC_{C5}	SOC_{S2}	SOC_{S5}
(a)													
R	0·35	0·35	-0·35	0·35	0·19	0·08	-0·26	-0·28	-0·13	-0·30	-0·26	-0·40	-0·40
SC	0·11	0·11	-0·11	0·11	0·27	0·70	0·24	0·79	-0·42	0·28	0·74	0·14	0·76
SL	0·51	0·51	-0·51	0·51	0·25	0·61	0·07	0·54	-0·43	0·06	0·50	-0·11	0·44
POC_C	-0·12	-0·12	0·12	-0·12	-0·38	-0·25	0·22	-0·10	0·23	0·24	-0·01	0·44	0·16
POC_L	0·45	0·45	-0·45	0·45	0·04	0·65	0·12	0·53	-0·44	0·08	0·53	-0·08	0·48
DOC_C	-0·19	-0·14	-0·15	0·04	0·01	-0·04	0·00	0·06	-0·17	0·07	-0·02	0·03	0·10
DOC_L	0·28	0·05	-0·05	-0·34	0·26	0·34	-0·22	0·23	0·13	-0·31	-0·30	-0·30	-0·26
TOC_L	0·45	0·45	-0·45	0·45	0·04	0·65	0·12	0·53	-0·44	0·08	0·53	-0·08	0·48
ER_2	-0·18	-0·18	0·18	-0·18	-0·16	-0·33	-0·30	-0·46	0·62	-0·32	-0·45	-0·09	-0·29
ER_5	-0·13	-0·13	0·13	-0·13	-0·12	-0·42	-0·05	-0·38	0·49	-0·03	-0·33	0·21	-0·15
(b)													
R	0·23	0·23	-0·23	0·23	0·30	0·30	-0·51	-0·40	0·46	-0·56	-0·54	-0·58	-0·49
SC	0·36	0·36	-0·36	0·36	0·39	-0·12	-0·27	-0·32	0·16	-0·13	-0·20	-0·19	-0·06
SL	0·40	0·40	-0·40	0·40	0·30	0·19	-0·49	-0·46	0·46	-0·49	-0·52	-0·53	-0·40
POC_C	-0·29	0·13	0·08	-0·17	0·34	0·20	-0·20	-0·25	-0·17	-0·17	-0·19	-0·09	-0·15
POC_L	0·17	0·08	-0·04	-0·03	0·22	0·27	-0·27	0·00	0·13	-0·24	-0·07	-0·26	-0·08
DOC_C	0·10	0·10	-0·10	0·10	-0·16	-0·03	0·02	-0·07	-0·16	-0·10	0·00	-0·06	-0·16
DOC_L	0·33	0·33	-0·33	0·33	0·30	-0·01	-0·20	-0·31	0·09	-0·28	-0·26	-0·32	-0·27
TOC_L	0·17	0·08	-0·04	-0·03	0·22	0·27	-0·27	0·00	0·13	-0·24	-0·07	-0·26	-0·08
ER_2	-0·08	-0·08	0·08	-0·08	0·40	0·25	-0·38	-0·32	0·17	-0·50	-0·33	-0·40	-0·50
ER_5	0·03	0·03	-0·03	0·03	0·26	0·06	-0·27	-0·38	0·18	-0·38	-0·35	-0·40	-0·35

Note: Runoff (*R*), sediment concentration (SC), soil losses (SL), particulate sediment organic carbon content and losses (POC_C; POC_L), dissolved organic carbon content and losses (DOC_C; DOC_L), sediment enrichment ratio (ER) in soil organic carbon compared to the bulk 0–0·02 m (ER_2) and 0–0·05 m (ER_5) soil, and the controls of event rainfall amount (RA), six minutes maximum rainfall intensity (RI_6), three days antecedent rainfall (AR_3), cumulative rain since onset of rainy season (CR), mean slope gradient (*S*), proportion of the soil surface under crusting (Crust), basal soil cover (Cov), top-soil clay content (Clay), soil bulk density (ρ_b), soil organic carbon content in the 0–0·02 and 0–0·05 m layers (SOC_{C2}; SOC_{C5}), soil organic carbon content in the 0–0·02 and 0–0·05 m layers (SOC_{C2}; SOC_{C5}) and associated SOC stocks (SOC_{S2}; SOC_{S5}).

was however of a similar order to the 9 Mg ha^{-1} yr^{-1} value found by Roose and Barthès (2006 and Martinez-Mena *et al.* (2012 under similar climatic conditions in the Mediterranean region but for tilled soils.

The present study pointed to soil losses expressed in gram per meter of plot width increased 4·2 fold from the 1-m to the 5-m long plots (23·2 versus 97·6 g m^{-1}, Table II). Such an increase in water erosion efficiency can be explained by an increase in flow velocity on the longer plots, resulting in an enhanced transportation of soil particles by rain-impacted flow (e.g. Kinnell, 2001).

Overall, runoff and soil losses were affected the most by slope gradient and soil clay content and soil bulk density, while rainfall characteristics and slope length had a more limited impact (Figure 3).

Significance of soil organic carbon losses by water erosion

POC_L computed over the 32 study events averaged 13·16 and 47·30 g C m^2 yr^{-1} for the respective 1- and 5-m long plots of this study, were in concordance with the range found in a review by Roose and Barthès (2006, in sub-humid Africa (36 g C m^2 yr^{-1}), but higher than rates observed in the Mediterranean (14 g C m^2 yr^{-1}).

At the 1-m slope length, the annual depletion rate of SOC stocks by RIF was as high as 0·9% when comparing it to the 0–0·05 m layer and 1·6% when comparing it to the 0·02 m topsoil layer. The annual losses in carbon stocks on 5-m long plots increased to 3·3%, when considering the 0–0·05 m layer, and to 5·8% in the case of 0–0·02 m, as RIF becomes more efficient. When the SOC stock was calculated for a depth of up to 0·3 m (average of 5·59 kg C m^2 computed from the five landscape positions and using data from Dlamini *et al.* [2011), the resultant annual SOC stock depletion rate was 0·23% on the 1-m and 0·85% on the 5-m plots. The SOC stock depletion rates calculated for the longer plots, corresponded with the findings of a study by Cogle *et al.* (2002 conducted in the semi-arid tropics of India, where a depletion rate of 0·5% was observed. Furthermore a study conducted by Chaplot *et al.* (2007 in the tropical humid climate of Laos, also publicized a slightly higher depletion rate of 1·3% for clayey soils under steep slope conditions. The depletion rates observed in this study were however much lower than the 16% found by Roose (1978 in Burkina Faso.

Overall, TOC_L were affected the most by rainfall characteristics (an increase with increasing CR, RA and RI_6), while slope length, slope gradient, soil crusting, soil clay content and soil bulk density did not seem to impact (Figure 3).

On the selectivity of soil organic carbon losses through water erosion

The eroded sediments of both, the 1- and 5-m long plots were systematically enriched in SOC, compared to the original bulk soil, confirming previous results of studies conducted on OC erosion by water (e.g. Gregorich *et al.*, 1998; Behre *et al.*, 2007; Muller-Nedbock and Chaplot, 2015). When using the top 0–0·3 m layer soil as a benchmark reference, RIF lead to the sediments becoming enriched in OC by a factor of between 3·2 and 3·9, dependent upon the length of the plot. Such ratios were similar to ones observed in Kenya (ER = 3·3; Boye and Albrecht, 2006) but appeared to be lower than those observed in cultivated fields of Burkina Faso (ER = 4·3; Bilgo *et al.*, 2006), in the sandy soils under maize cultivation in South Africa (4·3 < ER < 4·8; Mchunu *et al.*, 2011), and in the sandy,

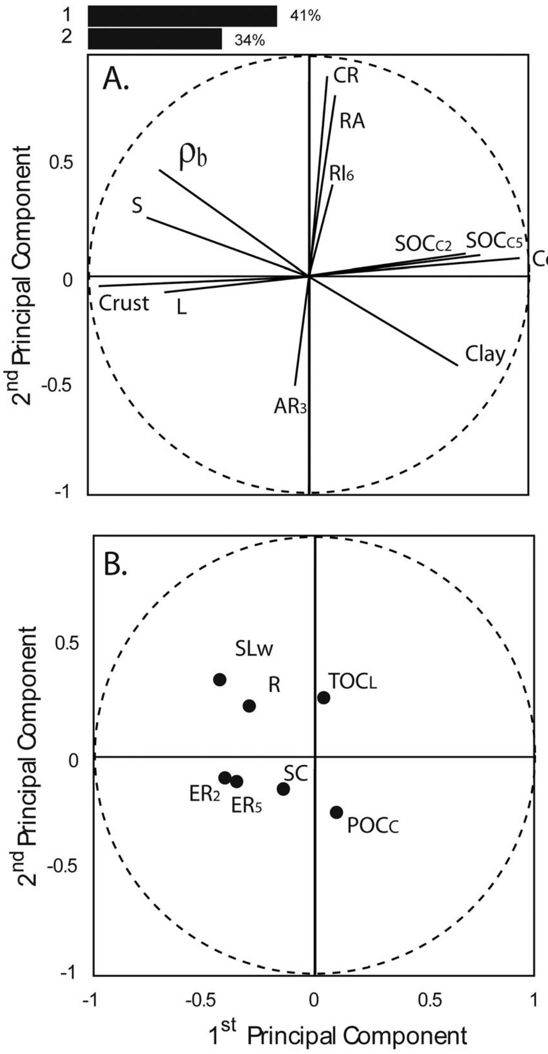

Figure 3. Display of the two first principal components of a principal component analysis (PCA) generated using the soil and environmental variables of event rainfall amount (RA), six-minutes maximum rainfall intensity (RI_6), three-days antecedent rainfall (AR_3), cumulative annual rainfall (CR), mean slope gradient (S), proportion of the soil surface under crusting (Crust), basal soil cover (Cov), top-soil clay content (Clay), soil bulk density (ρ_b), soil organic carbon content in the 0–0·02 and 0–0·05 m layers (SOC_{C2}; SOC_{C5}), soil organic carbon content in the 0–0·02 and 0–0·05 m layers (SOC_{C2}; SOC_{C5}) and associated SOC stocks (SOC_{S2}; SOC_{S5}), slope length (*L*) (A); position of the variables of soil and soil carbon erosion on the PCA axes (B): runoff (*R*), sediment concentration (SC), soil losses per plot meter width (SL_W), dissolved organic carbon content in runoff and losses (DOC_C; DOC_L), particulate organic carbon content in sediments (POC_C), total organic carbon losses (TOC_L), sediment enrichment ratio (ER) in soil organic carbon compared to the bulk 0–0·02 m (ER_2) and 0–0·05 m (ER_5) bulk soil.

semi-arid environments of Mali (ER = 10; Drissa *et al.*, 2004). Due to organic matter being lighter than soil minerals, preferential detachment and transport of the carbon-enriched top-soil occurs, and hence the eroded sediments are more likely to be enriched in SOC, in comparison to the original bulk soil. As pointed out by our results, the ER from 1-m long plots was found to be as low as 2·57 for the topmost 0·05 m and to 1·86 for the 0·02 m layer. Assuming that SOC is homogeneously distributed throughout the top 2 cm of soil, water erosion is responsible for detaching and transporting 86% more OC than mineral particles on the 1-m plots. This rate decreases to 61% on 5-m long plots, owing to the increasing RIF efficiency for soil particles detachment and transport on an increased slope length.

On the controls of soil organic carbon erosion

The positive correlation between rainfall amount, rainfall intensity and TOC_L was to be expected (Bryan, 2000; Kinnell, 2004; Jacinthe *et al.*, 2004; Parsons and Stone, 2006) because increased rain intensity accelerates soil saltation detachment and transportation. The increase in OC content with a decrease in rainfall intensity can be supported by the results of Jacinthe *et al.* (2004 and Martinez-Mena *et al.* (2012. Jacinthe *et al.* (2004 indicated that low-intensity winter storms yield more OC (37 g C kg^{-1}) and volatile carbon (30–40% total carbon) than high-intensity summer rain storms (22·1 g C kg^{-1} and 13%, respectively). In a study from the Spanish mainland, Martinez-Mena *et al.* (2012 pointed to a positive correlation between the erosion potential of rain (calculated as product of rainfall intensity and rainfall amount) and carbon concentration in sediment ($r = 0{\cdot}54$). Intense events enhance the raindrop erosion potential, accelerate overland flow erosion, and also contribute to soil erosion by disaggregating and saturating the soils. The consequence of this is a decrease in soil water infiltration, which in turn further enhances the efficiency of sheet erosion (Castillo *et al.*, 2003).

Our results (Table III) revealed that soil carbon losses increased with an increase in CR, but a decrease in AR_3, contrary to what was expected. This is likely to explain the lower particulate carbon erosion during the first half of the studied rain season, and the higher erosion rates with the consecutive events as cumulative rain increases and soils become saturated by water (Orchard *et al.*, 2013). On the contrary, as CR increased, DOC losses decreased, which is an already observed established trend (Gregorich *et al.*, 1998).

Soil losses and runoff increased with increasing slope length, which is a direct result of increased RIF efficiency as the overland flow efficiency increases (Kinnell, 2004). Moreover, on a steeper slope gradient, water has less time to infiltrate causing greater volumes to remain on the surface, resulting in more runoff, thus making possible RIF (Kinnell, 2004; Puigdefabregas *et al.*, 1999). Various field observations pointed out the presence of soil particle redistribution on longer runoff plots, resulting in the formation of sedimentary crusts with a diminished infiltration capacity (Maïga-Yaleu *et al.*, 2013), which renders an explanation for the greater runoff rate observed on the longer plots.

On the controls of soil organic carbon erosion selectivity

Roose and Barthès (2006 pointed towards a link between SOC enrichment of eroded sediment and land use. Revealing ER values below 1·1 for bare tilled soils and over 2·4 for 80% of the natural vegetation land use areas (i.e. forest, savanna, or fallow), the latter of which categories displaying a similar range as observed in the present study. Surprisingly, our study revealed no relationship between any rainstorm characteristics and the selectivity of water erosion for SOC losses, which contradicted Schiettecatte *et al.* (2008 laboratory results.

The present study also revealed significant increases in SOC enrichment levels of sediments with decreasing plot length and increasing clay content, SOC stocks and basal grass cover. The lower erosion selectivity for SOC on longer plots could be caused by differences in particle transport. Indeed, while splash has the potential to detach all soil particle sizes and densities from the soil, the finer and lighter fractions such as organic matter are more readily exported by associated shallow runoff, thus explaining the SOC enrichment. An accelerated runoff is able to transport a larger range of soil particle sizes, thus explaining a lower erosion selectivity potential. This is partly confirmed by a positive correlation between SOC enrichment and the overall soil losses, a result that has also been confirmed by Roose and Barthès (2006. The decrease in SOC selectivity with increasing soil clay and carbon content, a result previously demonstrated by Muller-Nedbock and Chaplot (2015) in a meta-analysis, might be a result of the erosion of the entire stable soil aggregates.

Conclusion

In this study in the hillslope of the Drakensberg foothills of South Africa, our main objective was to evaluate the impact of selected soil and environmental factors on the efficiency of sheet erosion to detach and transport SOC. Three main results were gained by monitoring runoff plots of 1- and 5-m long, from November 2010 up to February 2013:

1. Soil and SOC losses were about six times higher on the 5-m plots than on the 1-m ones. This revealed a sharp increase of RIF efficiency as slope length increases.
2. There was a general enrichment in SOC of the sediments compared to the original bulk soil (0–0·05 m), which slightly decreased with slope length, as RIF efficiency increased;
3. The selectivity of SOC erosion was influenced little by the characteristics of rainstorms but increased with soil crusting, and decreased with top-soil soil clay and carbon contents.

These results are expected to improve our understanding of SOC erosion from soils and its main controls, important, new knowledge that could be integrated into future erosion and carbon models. Further research should however be performed on both the quality of the eroded SOM and should consider the fate of the eroded carbon. While SOC is preferentially eroded, what proportion is redeposited in hillslopes or river basins? How much of the eroded carbon reaches the open ocean, and how much is emitted to the atmosphere? These are important questions which remain largely unanswered. Research studies should also consider the link between the selectivity of erosion for SOC and the replacement of the eroded carbon at former erosion sites and the reduced decomposition rates in depositional sites, which according to Behre *et al.* (2007 can largely compensate the carbon losses from soils when larger surface areas are considered.

Acknowledgements—This study was performed under the umbrella of the Water Research Commission of South Africa (K5/2266) and the Institut National des Sciences de l'Univers (EC2CO program; DESTOC project), which both focuses on nutrient and organic carbon losses from soils by water erosion and their fate to the ocean. The authors gratefully acknowledge the School of Agricultural, Earth and Environmental Sciences and the Farmer Support Group, University of KwaZulu-Natal, for providing support and assistance and the Institut de Recherche pour le Développement (IRD) for allowing this international collaboration. The authors also thank Cobus Pretorius and Jean-Louis Janeau for the conception and manufacturing of the plots and their installation; and the Potshini community for assistance in data collection and kindly allowing the research to be performed on their land. A final thanks to the two anonymous reviewers for the tremendous improvement of this paper.

References

Asadi H, Ghadiri H, Moussavi A, Rose CW. 2011. Flow-driven soil erosion processes and the size selectivity of sediment. *Journal of Hydrology* **406**: 73–81.

Behre A, Harte J, Harden J, Torn M. 2007. The significance of the erosion-induced terrestrial carbon sink. *BioScience* **57**: 337–346.

Biggelaar C, Lal R, Wiebe K, Breneman V. 2001. Impact of soil erosion on crop yields in North America. *Advances in Agronomy* **72**: 1–52.

Bilgo A, Serpantie G, Masse D, Fournier J, Hien V. 2006. Carbon, nitrogen, and fine particles removed by water erosion on crops, fallows, and mixed plots in Sudanese savannas (Burkina Faso). In Soil Erosion and Carbon Dynamics, Feller C, Roose EJ, Stewart BA, Barthes B, Lal R (eds). CRC Press: Boca Raton, FL; 125–142.

Boye A, Albrecht A. 2006. Soil erodibility, control and soil carbon losses under short-term tree fallows in western Kenya. In Soil Erosion and Carbon Dynamics, Feller C, Roose EJ, Stewart BA, Barthes B, Lal R (eds). CRC Press: Boca Raton, FL; 181–196.

Bryan R. 2000. Soil erodibility and processes of water erosion on hillslope. *Geomorphology* **32**: 385–415.

Castillo V, Gòmez-Plaza A, Martinez-Mena A. 2003. The role of antecedent soil water content in the runoff response of semiarid catchments: a simulation approach. *Journal of Hydrology* **284**: 114–130.

Chaplot V. 2013. Impact of terrain attributes, parent material and soil types on gully erosion. *Geomorphology* **186**: 1–11.

Chaplot V, Le Bissonnais Y. 2003. Runoff features for interrill erosion at different rainfall intensities, slope lengths and gradients in an agricultural loessial hillslope. *Soil Science Society of America Journal* **67**: 844–851.

Chaplot V, Poesen J. 2012. Sediment, soil organic carbon and runoff delivery at various spatial scales. *Catena* **88**: 46–56.

Chaplot V, Rumpel C, Valentin C. 2005. Water erosion impact on soil and carbon redistributions within the Mekong basin. *Global Biogeochemical Cycles* **19**: 20–32. DOI:http://dx.doi.org/10.1029/2005GB002493.

Chaplot V, Khampaseuth X, Valentin C, Le Bisonnais Y. 2007. Interrill erosion in the sloping lands of northern Laos submitted to shifting cultivation. *Earth Surface Processes and Landforms* **32**: 415–428.

Cogle A, Rao K, Yule D, Smith G, George P, Srinivasan S, Jangawad L. 2002. Soil management for alfisols in the semiarid tropics: erosion, enrichment ratios and runoff. *Soil Use and Management* **18**: 10–17.

Dlamini P, Orchard C, Jewitt G, Lorentz S, Tishall L, Chaplot V. 2011. Quantifying interrill erosion in a sloping-land-agricultural catchment of KwaZulu Natal, South Africa. *Agriculture Water Management* **98**: 1711–1718.

Drissa D, Orange D, Roose E. 2004. Influence des pratiques culturales et du type de sols sur les stocks et pertes de carbone par érosion en zone soudanienne du Mali. In Soil Erosion and Carbon Dynamics, Feller C, Roose EJ, Stewart BA, Barthes B, Lal R (eds). CRC Press: Boca Raton, FL; 193–207.

Gee GW, Bauder JW. 1986. Particle-size analysis. In Methods of Soil Analysis, Part 1. Physical and Mineralogical Methods, Klute A (ed), 2nd edn. Soil Science Society of America: Madison, WI; 383–411.

Govers G. 1985. Selectivity and transport capacity of thin flows in relation to rill erosion. *Catena* **12**: 35–49.

Govers G. 1990. Empirical relationships for the transporting capacity of overland flow. *International Association of Hydrological Sciences Publication* **189**: 45–63.

Gregorich E, Greer K, Anderson D, Liang B. 1998. Carbon distribution and losses: erosion and deposition effects. *Soil and Tillage Research* **47**: 291–302.

Hairsine PB, Rose CW. 1991. Rainfall detachment and deposition – sediment transport in the absence of flow-driven processes. *Soil Science Society of America Journal* **55**: 320–324.

Hoffmann T, Mudd SM, van Oost K, Verstraeten G, Erkens G, Lang A, Middelkoop H, Boyle J, Kaplan J, Willenbring J, Aalto R. 2013. Short Communication: Humans and the missing C-sink: erosion and burial of soil carbon through time. *Earth Surface Dynamics* **1**: 45–52.

Jacinthe P, Lal R. 2001. A mass balance approach to assess carbon dioxide evolution during erosional events. *Land Degradation and Devastation* **12**: 329–339.

Jacinthe PA, Lal R, Owens LB, Hothem DL. 2004. Transport of labile carbon in runoff as affected by land use and rainfall characteristics. *Soil and Tillage Research* **77**: 111–123.

Jambu M. 1991. Exploratory and Multivariate Data Analysis. Academic: Orlando, FL.

Kinnell P. 2001. Comments and letters to the editor: comments on vertical hydraulic gradient and run-on water and sediment effects on erosion processes and sediment regimes. *Soil Science Society of America* **65**: 953–954.

Kinnell P. 2004. Raindrop-impact-induced erosion processes and prediction: a review. *Hydrological Processes* **19**: 2815–2844.

Lal R. 2003. Soil erosion and the global carbon budget. *Environment International* **29**: 437–450.

Lal R. 2004. Soil carbon sequestration to mitigate climate change. *Geoderma* **123**: 1–22.

Maïga-Yaleu S, Guiguemde I, Yacouba H, Karambiri H, Ribolzi O, Bary A, Ouedraogo R, Chaplot V. 2013. Soil crusting impact on soil organic carbon losses by water erosion. *Catena* **107**: 26–34.

Martinez-Mena M, Lopez J, Almagro M, Albaladejo J, Castillo V, Ortiz R, Fayos B. 2012. Organic carbon enrichment in sediments: effects of rainfall characteristics under different land uses in a Mediterranean area. *Catena* **94**: 36–42.

Mchunu C, Chaplot V. 2012. Land degradation impact on soil carbon losses through water erosion and CO_2 emissions. *Geoderma* **178**: 72–79.

Mchunu C, Manson A, Jewitt G, Lorentz S, Chaplot V. 2011. No-till impact on soil and soil organic carbon erosion under crop residues scarcity in South Africa. *Soil Science Society of America Journal* **75**: 1503–1512.

Mitchell JK, Mostaghimi S, Pound M. 1983. Primary particle and aggregate size distribution of eroded soil from sequenced rainfall events. *Transactions of ASAE* **26**: 1773–1777.

Muller-Nedbock D, Chaplot V. 2015. Soil carbon losses by sheet erosion: a potentially critical contribution to the global carbon cycle. *Earth Surface Processes and Landforms* **40**, 1803–1813.

Nadeu E, de Vente J, Martínez-Mena M, Boix-Fayos C. 2011. Exploring particle size distribution and organic carbon pools mobilized by different erosion processes at the catchment scale. *Journal of Soils and Sediments* **11**: 667–678.

Nadeu E, Behr AA, de Vente J, Boix-Fayos C. 2012. Erosion, deposition and replacement of soil organic carbon in Mediterranean catchments: a geomorphological, isotopic and land use change approach. *Biogeosciences* **9**: 1099–1111.

Orchard C, Lorentz S, Jewitt G, Chaplot V. 2013. Spatial and temporal variations of overland flow at the microcatchment level. *Hydrological Processes* **27**: 2325–2338. DOI:http://dx.doi.org/10.1002/hyp.9217.

Parsons A, Stone P. 2006. Effects of intra-storm variations in rainfall intensity on interrill runoff and erosion. *Catena* **67**: 68–78.

Pimentel D, Harvey C, Resosudarmo P, Sinclair K, Kurz D, McNair M, Crist S, Shpritz L, Fitton L, Saffouri R, Blair R. 1995. Environmental and economic costs of soil erosion and conservation benefits. *Science* **267**: 1117–1123.

Poesen J, Savat J. 1980. Particle-size separation during erosion by splash and runoff. In Assessment of Erosion, de Boodt M, Gabriels D (eds). John Wiley & Sons: Chichester; 427–439.

Puigdefabregas J, Sole A, Gutierrez L, del Barrio G, Boer M. 1999. Scales and processes of water and sediment redistribution in drylands: results from the Rambla Honda field site in southeast Spain. *Earth-Science Reviews* **48**: 39–70.

Rodríguez-Rodríguez A, Guerra A, Arbelo C, Mora JL, Gorrín SP, Armas C. 2004. Forms of eroded soil organic carbon in Andosols of the Canary Islands (Spain). *Geoderma* **121**: 205–219.

Roose E. 1978. Dynamique actuelle de deux sols ferrugineux tropicaux indurés sous sorgho et sous savane Soudano-Sahélienne-Saria (Haute-Volta): Synthèse des campagnes 1971–1974. ORSTOM Publisher: Paris.

Roose E, Barthès B. 2006. Soil carbon erosion and its selectivity at the plot scale in tropical and Mediterranean regions. In Soil Erosion and Carbon Dynamics, Feller C, Roose EJ, Stewart BA, Barthes B, Lal R (eds). CRC Press: Boca Raton, FL; 55–72.

Schiettecatte W, Gabriels D, Cornelis WM, Hofman G. 2008. Enrichment of organic carbon in sediment transport by interrill and rill erosion processes. *Soil Science Society of America Journal* **72**: 50–55.

Schlesinger W, Andrews J. 2000. Soil respiration and the global carbon cycle. *Biogeochemistry* **48**: 7–20.

Van Hemelryck H, Govers G, Van Oost K, Merckx R. 2011. Evaluating the impact of soil redistribution on the in situ mineralization of soil organic carbon. *Earth Surface Processes and Landforms* **36**: 427–438.

Wang Z, Govers G, Steegen A, Clymans W, Van den Putte A, Langhans C, Merckx R, Van Oost K. 2010. Catchment-scale carbon redistribution and delivery by water erosion in an intensively cultivated area. *Geomorphology* **124**: 65–74.

World Reference Base for Soil Resources (WRB). 2006. World Soil Resources Reports, No. 696 103. FAO: Rome.